Наносистеми, наноматеріали, нанотехнології
Nanosistemi, Nanomateriali, Nanotehnologii
2024, т. 22, № 2, сс. 367–378
https://doi.org/10.15407/nnn.22.02.367

PACS numbers: 61.72.Ff, 61.80.Ed, 68.37.Hk, 81.07.Pr, 82.35.Np, 83.60.Np, 87.64.M-

Effect of SiO_2–SnO_2 Nanofiller on the Characteristics of Biopolymer Blend and Its Application as Gamma-Ray Shielding

Rehab Shather Abdul Hamza and Majeed Ali Habeeb

College of Education for Pure Sciences,
Department of Physics,
University of Babylon,
Hillah, Iraq

In this paper, the synthesis of novel (polyvinyl alcohol (PVA) and carboxymethyl cellulose (CMC)/silicon dioxide (SiO_2) and tin oxide (SnO_2)) nanocomposites to apply for gamma-ray shielding with low unit cost, flexible, lightweight, and high corrosion resistance. Scanning electron microscopy analysis of the nanocomposites consisting of PVA–CMC–SiO_2–SnO_2 films reveals the presence of numerous aggregates or fragments, which exhibit the consistent and coherent distribution on the upper surface. The optical microscope analysis of the blend additive distribution of nanoparticles indicates the uniform and homogeneous pattern. The prepared nanocomposites underwent testing to evaluate their effectiveness in shielding against gamma-rays. The experimental findings indicate that the nanocomposite films of PVA–CMC–SiO_2–SnO_2 exhibit significant attenuation levels for gamma-rays.

У цій роботі розглянуто синтезу нових нанокомпозитів (полівініловий спирт (ПВС) та карбоксиметилцелюлоза (КМЦ)/діоксид Силіцію (SiO_2) та оксид Стануму (SnO_2)) задля застосування для екранування γ-променів з низькою вартістю одиниці, гнучкістю, легкістю та високою корозійною стійкістю. Сканувальна електронно-мікроскопічна аналіза нанокомпозитів, що складаються з плівок ПВС–КМЦ–SiO_2–SnO_2, виявляє наявність численних аґреґатів або фраґментів, які демонструють послідовний і когерентний розподіл на верхній поверхні. Аналіза за допомогою оптичного мікроскопа адитивного розподілу наночастинок у суміші вказує на рівномірну й однорідну структуру. Підготовлені нанокомпозити пройшли випробування для оцінки їхньої ефективности в екрануванні від γ-променів. Експериментальні результати свідчать про те, що нанокомпозитні плівки ПВС–КМЦ–SiO_2–SnO_2 демонструють значні рівні ослаблення γ-променів.

Key words: nanocomposites, SiO_2–SnO_2 nanoparticles, polyvinyl alcohol,

carboxymethyl cellulose, structural properties, gamma-rays.

Ключові слова: нанокомпозити, наночастинки SiO_2–SnO_2, полівініловий спирт, карбоксиметилцелюлоза, структурні властивості, γ-промені.

(Received 11 July, 2023)

1. INTRODUCTION

Polymeric materials are widely utilized in contemporary applications due to their affordability, ease of production, favourable properties, and frequently exceptional performance. It is widely acknowledged that most polymeric materials exhibit insulating properties, rendering them suitable for electrical and electronic use; a relationship has been established since antiquity. Polymeric materials have become a fundamental component in the electrical and electronic industries due to their advantageous characteristics, despite initially being utilized as auxiliary materials [1].

A polymer blend refers to the amalgamation of two or more polymers, creating a novel material exhibiting diverse physical characteristics. The utilization of heat in conjunction with thermoplastic materials and the combination of heat and plastic materials has been a subject of interest in various fields. The five primary classifications of polymer blends are polymer-filling blends, mixtures, and rubber-thermosetting blends. The practice of polymer blending has garnered significant interest due to its inherent advantages in terms of simplicity and cost-effectiveness, making it a viable approach for producing scalable polymeric materials with the potential for widespread commercial utilization. Simply put, mixtures' properties can be controlled based on their intended use through the appropriate selection of polymer materials [2, 3].

Polymer nanocomposites (PNCs) are determined as a type of material with unique properties. A polymer nanocomposite (PNC) is a polymer- or copolymer-containing nanoparticles or nanofillers distributed throughout the polymer matrix. Inorganic particles are disseminated in an organic polymer matrix in at least one dimension to improve the quality attributes of the material [4, 5]. PNCs are modern polymers, which can be used instead of traditional filled polymers. One of the notable enhancements observed in nanocomposites is the significant improvement in their properties compared to those of pure polymers. This improvement can be attributed to the enhanced dispersion of fillers within the nanocomposite structure. The enhancements include heightened tensile strength, enhanced electrical conductivity, decreased flammability, and improved thermal stability. Nanoparticles added to polymer composites also re-

sulted in a new line of composite materials with improved and unique properties. Platelets, fibres, and spheroids are examples of these ones [6, 7].

Polyvinyl alcohol (PVA) is a polymer with remarkable characteristics, including biodegradability, non-toxicity, biocompatibility, water solubility, and non-carcinogenicity. It can form hydrogels through either chemical or physical means [8, 9]. PVA exhibits a sufficiently high tensile strength and demonstrates sufficient flexibility. In order to enhance deformability, PVA is commonly subjected to plasticization through various low molecular weight compounds, predominantly characterized by polar groups [10, 11].

Carboxymethyl cellulose (CMC) is cellulose ether that gels at high temperatures and forms excellent films. Due to its polymeric composition and substantial molecular weight, it possesses the potential to serve as filler in biocomposite films. The incorporation of CMC can lead to improvements in both the mechanical and barrier characteristics of starch-based films. Cellulose is a linear, high molecular weight detergent and surfactant used as a polymer antidirt agent and a safe, reusable, and biodegradable fibre surface protection [12, 13].

Silicon oxide (SiO_2) or silica is most common in nature as quartz. It has many forms, but all forms of silica are identical in chemical composition, but with different atomic arrangements. Silica, in all its manifestations, exists as an odourless solid material consisting of silicon and oxygen atoms. Silica particles can become airborne and aggregate to form dust that lacks explosive properties [14, 15].

Tin oxide (SnO_2) is a transparent conducting oxide that increasingly attracts attention as a nanostructured material, primarily due to its remarkable electrical and optical characteristics. Tin dioxide (SnO_2) has emerged as a highly-promising material for various applications, future optoelectronic devices, photocatalysis, and solar cells. This phenomenon can be attributed to the significant transmittance exhibited by the material within the visible range of the electromagnetic spectrum, coupled with a conductivity range typically falling between 10^2–10^3 $(\Omega \cdot cm)^{-1}$ [16, 17]. Owing to its non-toxic nature, affordability, chemical reactivity, and thermal resilience, this material has been extensively utilised in biomedical applications and gas sensing [18, 19].

Gamma-radiation is of particular significance regarding external exposure due to its substantial penetrating capability and potential adverse effects on human health. The cumulative exposure to ionizing radiation, such as gamma-rays, is associated with various adverse health effects, including the development of cancer, DNA mutations, and infertility, among others. Nevertheless, the ramifications of these exposures are contingent upon several variables, encompassing the specific type of radiation and its corresponding en-

ergy, the quantity of administered dose (referred to as absorbed dose), and the duration of exposure. The prioritization of shielding has become imperative to safeguard individuals and equipment, owing to the escalating utilization of radioactive substances in medicine and industry [20, 21].

2. EXPERIMENTAL PART

Nanoparticles of silicon dioxide (SiO_2) and tin oxide (SnO_2) were incorporated into nanocomposite films at different weight percentages (0, 2, 4, 6, and 8 wt.%), using the casting method. The procedure entailed dissolving pure polyvinyl alcohol (PVA) and carboxymethyl cellulose (CMC) in a ratio of 68:32 in 40 ml of distilled water for 40 minutes under constant stirring, using a magnetic stirrer at a temperature of 70°C to attain a more uniform solution; this one led to the formation of nanocomposite films consisting of PVA, CMC, silicon dioxide (SiO_2), and tin dioxide (SnO_2). The liquid was contained within a Petri dish. After synthesising polymer mixture nanocomposites, the resulting solution underwent a four-day drying period at ambient temperature. The NCs were extracted from the Petri dish and utilized for measurement.

The surface characteristics of the PVA–CMC–SiO_2–SnO_2 nanocomposites were examined through the utilization of a scanning electron microscope (Model/Mira-3 — Details/1.2 nm at 30 kV; 2.3 nm at 3 kV — Manufacturing and Country/Tescan, France) and an Olympus type Nikon-73346 optical microscope with a magnifying power of ×10 and a camera for microscopic photography. This study examines the gamma-ray attenuation characteristics of SiO_2–SnO_2 nanoparticles with different volume fractions, utilizing nanocomposites for gamma-ray shielding. Prior to exposure to a collimated beam emanating from gamma-ray sources (specifically Cs-137 with an activity of 5 mci), specimens were situated in a designated location. The distance between the gamma-ray source and the detector is of 2 cm. The current investigation entailed the determination of linear attenuation coefficients using Geiger counter measurements. The study assessed gamma-ray fluxes transmitted through nanocomposites of NCs composed of PVA–CMC–SiO_2–SnO_2.

The equation presented below can be used to derive the linear attenuation coefficient μ based on the material thicknesses [22, 23]:

$$N = N_0 e^{-\mu x}, \tag{1}$$

The variable N_0 represents the number of radiation particles detected within a specific time interval without any absorber. Meanwhile, the variable μ denotes the attenuation coefficient of gamma-

radiation. Lastly, the variable N signifies the number of radiation particles detected within the same time interval but with a sample of thickness x.

3. RESULTS AND DISCUSSIONS

3.1. Scanning Electron Microscope Measurements of PVA–CMC–SiO_2–SnO_2 NCs

To examine the spatial arrangement of micro-nanofillers in the nanocomposite samples, scanning electron microscopy (SEM) images were acquired. Figure 1 displays the scanning electron microscopy (SEM) images of the pure and nanocomposite samples. The homogenous dispersion of SiO_2–SnO_2 nanoparticles in the polymeric samples can be observed in Figs. 1, *b*, *c*. The scanning electron microscopy (SEM) images of the doped samples reveal the presence of white granules and the random distribution of granule clusters on the surfaces of the samples. Furthermore, upon examination of the images, it is evident that the distribution of SiO_2 and SnO_2 on the surfaces of the samples is uniform [24–28].

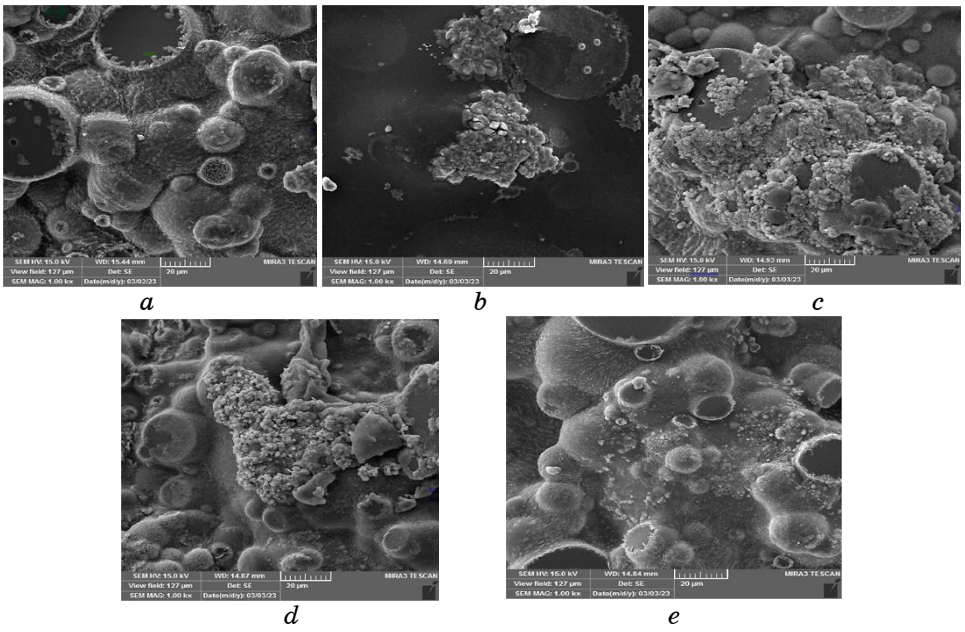

Fig. 1. SEM images of PVA–CMC–SiO_2–SnO_2) NCs: (*a*) PVA–CMC; (*b*) 2 wt.% SiO_2–SnO_2; (*c*) 4 wt.% SiO_2–SnO_2; (*d*) 6 wt.% SiO_2–SnO_2; (*e*) 8 wt.% SiO_2–SnO_2.

Moreover, it has been demonstrated that the SiO_2–SnO_2 nanofillers, after modification, exhibit exceptional adhesion properties and establish robust interfacial bonding with the polymeric matrix. The observation of granule aggregation on the surfaces of the sam-

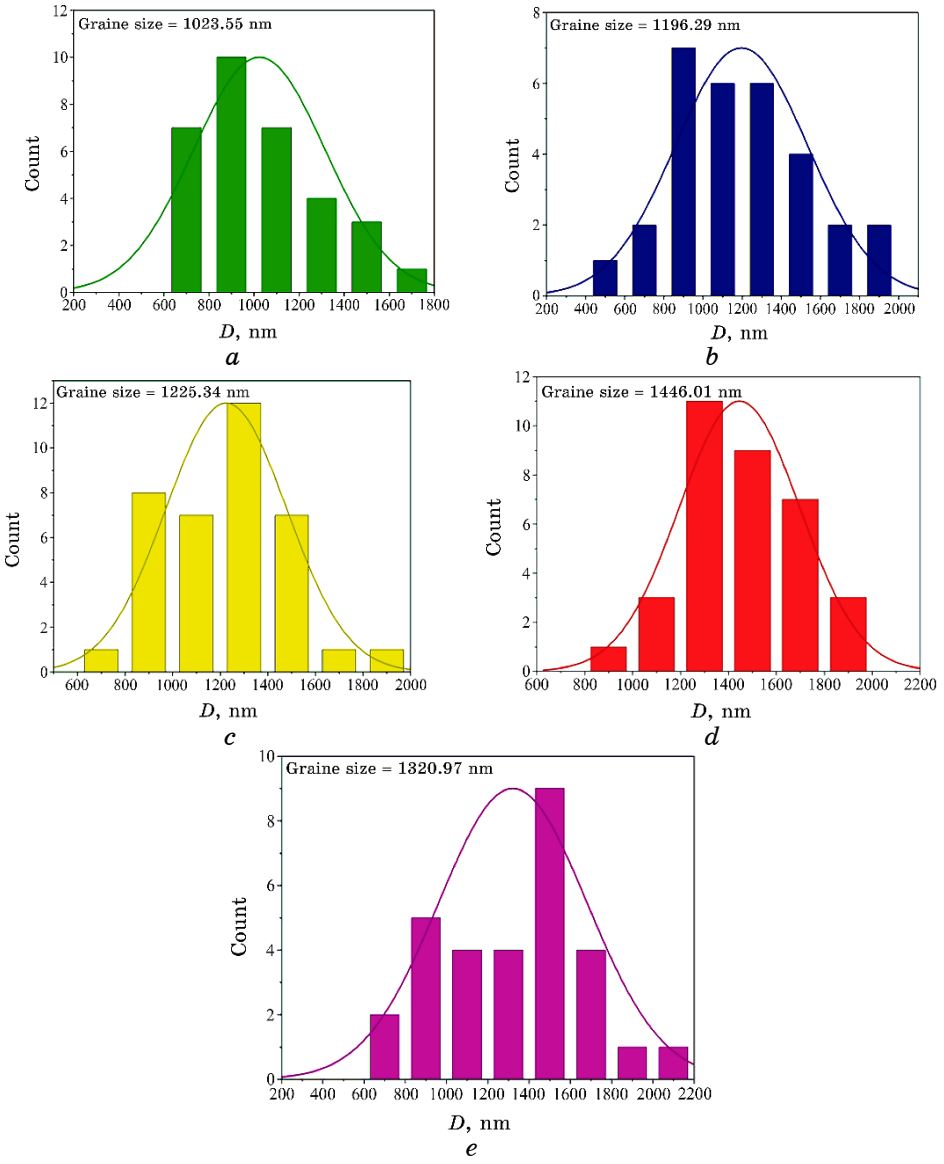

Fig. 2. Grain size for PVA–CMC–SiO_2–SnO_2 NCs: (*a*) PVA–CMC; (*b*) 2 wt.% SiO_2–SnO_2; (*c*) 4 wt.% SiO_2–SnO_2; (*d*) 6 wt.% SiO_2–SnO_2; (*e*) 8 wt.% SiO_2–SnO_2.

ples can be attributed to the complexation between the SiO_2–SnO_2 nanoparticles and the polymer, particularly at higher concentrations, as depicted in Figs. 1, *d*, *e*. The observed morphological alterations in the PVA–CMC composite suggest interactions between the nanofiller and polymer; this indicates that the constituent elements of the polymeric samples in the nanocomposite exhibit compatibility [29–33]. Figure 2 shows the grain size for PVA–CMC–SiO_2–SnO_2 nanocomposites calculated from SEM images.

3.2. Optical Microscope for PVA–CMC–SiO_2–SnO_2 NCs

Figure 3 shows the optical images of PVA–CMC–SiO_2–SnO_2 nanocomposites with different concentrations of SiO_2–SnO_2 nanoparticles at magnification power ×10. The present study involved a comparative analysis between pure polymer films and PVA–CMC–SiO_2–SnO_2 nanocomposite films. The microscopic images exhibit a discernible distinction among the samples as the proportions of SiO_2–SnO_2 nanoparticles are progressively increased, as visually depicted in images *a*, *b*, *c*, *d*, and *e*. Homogenous distribution of SiO_2–SnO_2 nanoparticles through PVA–CMC blend was observed. Upon reaching a concentration of 8 wt.% in polyvinyl alcohol films, SiO_2–SiO_2 nano-

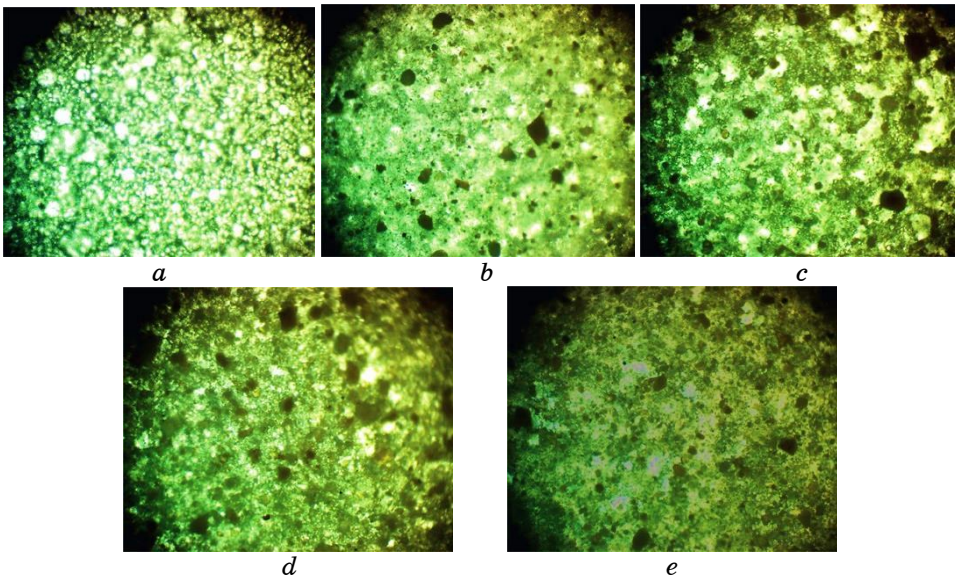

Fig. 3. Optical microscope images of PVA–CMC–SiO_2–SnO_2 NCs at a magnification (×10): (*a*) PVA–CMC; (*b*) 2 wt.% SiO_2–SnO_2; (*c*) 4 wt.% SiO_2–SnO_2; (*d*) 6 wt.% SiO_2–SnO_2; (*e*) 8 wt.% SiO_2–SnO_2.

particles transition to form a cohesive network within the polymer matrix [34–38].

3.3. Application of PVA–CMC–SiO_2–SnO_2 NCs for Gamma-Ray Shielding

Figure 4 illustrates the fluctuation of N/N_0 in the PVA–CMC blend, when exposed to varying concentrations of SiO_2–SnO_2 nanoparticles. The N/N_0 values exhibit a decrease as the ratio of SiO_2–SnO_2 nanoparticles increases. This observed behaviour could be attributed to the nanocomposite shielding materials' absorption or reflection of gamma-radiation [39–42]. Figure 5 shows increasing $\ln(N/N_0)$ of the PVA/CMC mixture with increases of SiO_2–Cr_2O_3 NPs concentrations [43].

Figure 6 illustrates the fluctuation in attenuation coefficients of gamma-radiation for the PVA–CMC blend about the concentrations of SiO_2–SnO_2 nanoparticles. The polymer blend demonstrated a favourable capacity for radiation absorption. The attenuation coefficients rise with increasing SiO_2–SnO_2 nanoparticles because shielding materials are made of nanocomposites, which either absorb or reflect gamma-rays [44, 45]. The attenuation coefficient of gamma-radiation for nanocomposites has reached a value of 0.026 cm^{-1}. Nevertheless, incorporating PVA–CMC–SiO_2–SnO_2 nanocomposites offer a distinct advantage due to their enhanced mobility and reduced electrical properties. The utilization of this technology does not result in any discernible impact on the magnetic or electrical

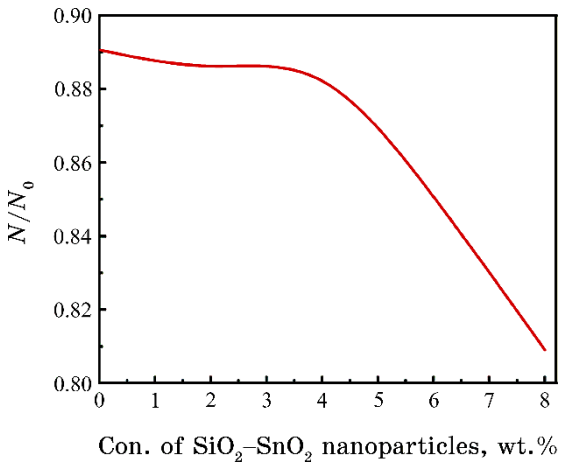

Fig. 4. Variance of N/N_0 for PVA/CMC mixture with different SiO_2/SnO_2 NPs concentrations.

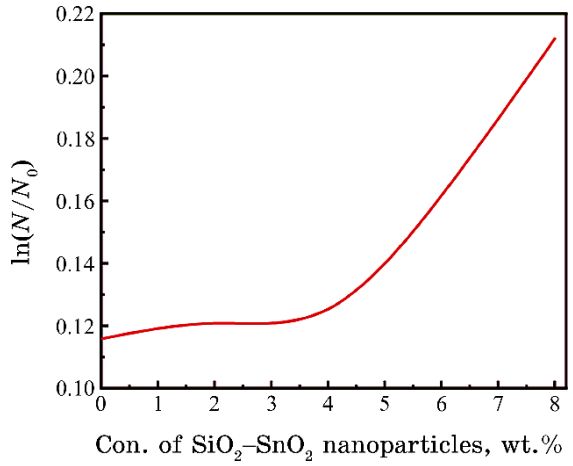

Fig. 5. Change of $\ln(N/N_0)$ for PVA/CMC blend with different concentrations of SiO_2/SnO_2 nanoparticles.

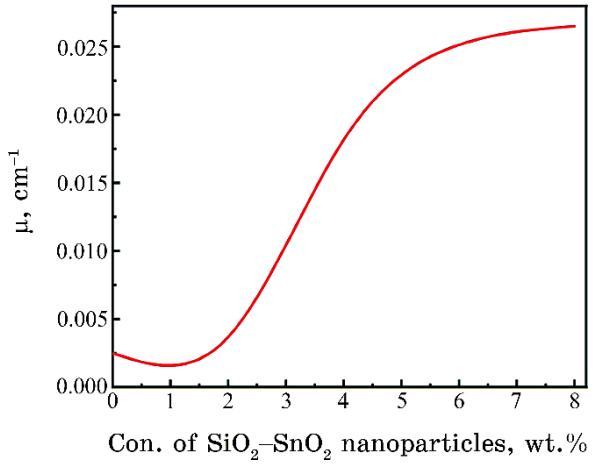

Fig. 6. Variance of attenuation coefficients of gamma-radiation for PVA/CMC blend with different concentrations of SiO_2/SnO_2 nanoparticles.

fields that may affect the health of individuals using or receiving treatment [46, 47].

4. CONCLUSIONS

The present study involved the production of plastic nanocomposite films utilizing the casting solution fabrication method. The films were fabricated using nanoparticles of silicon dioxide (SiO_2) and tin

oxide (SnO_2) in conjunction with polyvinyl alcohol (PVA) and carboxymethyl cellulose (CMC). The top surface of the PVA–CMC–SiO_2–SnO_2-NCs films was subjected to SEM analysis to investigate their surface morphology. The results suggest the presence of diverse fragments or conglomerates that were distributed stochastic across the surface. The optical microscope images reveal the emergence of a cohesive network after the creation of silicon dioxide (SiO_2) and tin oxide (SnO_2) nanoparticles in a polymer mixture, with a weight concentration of eight percent. The concentration of SiO_2–SnO_2 nanoparticles directly correlates with the attenuation coefficient of gamma-radiation, as observed by the concentration of NPs.

REFERENCES

1. A. A. ElBellihi, W. A. Bayoumy, E. M. Masoud, and M. A. Mousa, *Bulletin of the Korean Chemical Society*, **33**, No. 9: 2949 (2012); https://doi.org/10.5012/bkcs.2012.33.9.2949
2. M. A. Habeeb, *European Journal of Scientific Research*, **57**, No. 3: 478 (2011).
3. E. M. Masoud, *Ionics*, **25**: 2645 (2019); https://doi.org/10.1007/s11581-018-2802-1
4. M. A. Habeeb and Z. S. Jaber, *East European Journal of Physics*, **4**: 176 (2022); doi:10.26565/2312-4334-2022-4-18
5. A. H. Hadi and M. A. Habeeb, *Journal of Mechanical Engineering Research and Developments*, **44**, No. 3: 265 (2021); https://jmerd.net/03-2021-265-274
6. Q. M. Jebur, A. Hashim, and M. A. Habeeb, *Egyptian Journal of Chemistry*, **63**: 719 (2020); https://dx.doi.org/10.21608/ejchem.2019.14847.1900
7. O. B. L. López, G. L. Sierra, and G. A. I. Mejía, *Polymer Engineering & Science*, **39**, No. 8: 1346 (1999); https://doi.org/10.1002/pen.11523
8. S. M. Mahdi and M. A. Habeeb, *Optical and Quantum Electronics*, **54**, Iss. 12: 854 (2022); https://doi.org/10.1007/s11082-022-04267-6
9. N. Hayder, M. A. Habeeb, and A. Hashim, *Egyptian Journal of Chemistry*, **63**: 577 (2020); doi:10.21608/ejchem.2019.14646.1887
10. M. Marikkannan, V. Vishnukanthan, A. Vijayshankar, J. Mayandi, and J. M. Pearce, *AIP Advances*, **5**, No. 2: 027122 (2015); https://doi.org/10.1063/1.4909542
11. M. A. Habeeb, A. Hashim, and N. Hayder, *Egyptian Journal of Chemistry*, **63**: 709 (2020); https://dx.doi.org/10.21608/ejchem.2019.13333.1832
12. A. Hashim, M.A. Habeeb, and Q. M. Jebur, *Egyptian Journal of Chemistry*, **63**: 735 (2020); https://dx.doi.org/10.21608/ejchem.2019.14849.1901
13. S. M. Mahdi and M. A. Habeeb, *Physics and Chemistry of Solid State*, **23**, No. 4: 785 (2022); doi:10.15330/pcss.23.4.785-792
14. N. H. El Fewaty, A. El Sayed, R. Hafez, *Polymer Science Series A*, **58**: 1004 (2016); https://doi.org/10.1134/S0965545X16060055
15. M. A. Habeeb and W. S. Mahdi, *International Journal of Emerging Trends in Engineering Research*, **7**, No. 9: 247 (2019);

doi:10.30534/ijeter/2019/06792019
16. M. A. Habeeb and R. S. Abdul Hamza, *Journal of Bionanoscience*, **12**, No. 3: 328 (2018); https://doi.org/10.1166/jbns.2018.1535
17. S. Nambiar and J. T. Yeow, *ACS Applied Materials & Interfaces*, **4**, No. 11: 5717 (2012); https://doi.org/10.1021/am300783d
18. M. A. Habeeb, A. Hashim, and N. Hayder, *Egyptian Journal of Chemistry*, **63**: 697 (2020); https://dx.doi.org/10.21608/ejchem.2019.12439.1774
19. M. A. Habeeb and W. K. Kadhim, *Journal of Engineering and Applied Sciences*, **9**, No. 4: 109 (2014); doi:10.36478/jeasci.2014.109.113
20. M. Hdidar, S. Chouikhi, A. Fattoum, M. Arous, and A. Kallel, *Journal of Alloys and Compounds*, **750**: 375 (2018); https://doi.org/10.1016/j.jallcom.2018.03.272
21. M. A. Habeeb, *Journal of Engineering and Applied Sciences*, **9**, No. 4: 102 (2014); doi:10.36478/jeasci.2014.102.108
22. H. J. Park, A. Badakhsh, I. T. Im, M.-S. Kim, and C. W. Park, *Applied Thermal Engineering*, **107**: 907 (2016); https://doi.org/10.1016/j.applthermaleng.2016.07.053
23. S. M. Mahdi and M. A. Habeeb, *Digest Journal of Nanomaterials and Biostructures*, **17**, No. 3: 941 (2022); https://doi.org/10.15251/DJNB.2022.173.941
24. G. A. Eid, A. Kany, M. El-Toony, I. Bashter, and F. Gaber, *Arab. J. Nucl. Sci. Appl.*, **46**, No. 2: 226 (2013).
25. A. H. Hadi and M. A. Habeeb, *Journal of Physics: Conference Series*, **1973**, No. 1: 012063 (2021); doi:10.1088/1742-6596/1973/1/012063
26. Q. M. Jebur, A. Hashim, and M. A. Habeeb, *Egyptian Journal of Chemistry*, **63**, No. 2: 611 (2020); https://dx.doi.org/10.21608/ejchem.2019.10197.1669
27. G. Aras, E. L. Orhan, I. F. Selçuk, S. B. Ocak, and M. Ertuğrul, *Procedia–Social and Behavioral Sciences,* **95**: 1740 (2015); https://doi.org/10.1016/j.sbspro.2015.06.295
28. M. A. Habeeb and A. H. Mohammed, *Optical and Quantum Electronics*, **55**, Iss. 9: 791 (2023); https://doi.org/10.1007/s11082-023-05061-8
29. M. H. Dwech, M. A. Habeeb, and A. H. Mohammed, *Ukr. J. Phys.*, **67**, No. 10: 757 (2022); https://doi.org/10.15407/ujpe67.10.757
30. S. M. Mahdi and M. A. Habeeb, *Polymer Bulletin*, **80**: 12741 (2023); https://doi.org/10.1007/s00289-023-04676-x
31. M. Martin, N. Prasad, M. M. Siva lingam, D. Sastikumar, and B. Karthikeyan, *Journal of Material Science: Material in Electronics*, **29**: 365 (2018); https://doi.org/10.1007/s10854-017-7925-z
32. M. A. Habeeb and W. H. Rahdi, *Optical and Quantum Electronics*, **55**, Iss. 4: 334 (2023); https://doi.org/10.1007/s11082-023-04639-6
33. A. A. Mohammed and M. A. Habeeb, *Silicon*, **15**: 5163 (2023); https://doi.org/10.1007/s12633-023-02426-2
34. R. Dalven and R. Gill, *J. Appl. Phys.*, **38**, No. 2: 753 (1967); doi:10.1063/1.1709406
35. N. K. Al-Sharifi and M. A. Habeeb, *Silicon*, **15**: 4979 (2023); https://doi.org/10.1007/s12633-023-02418-2
36. R. N. Bhagat and V. S. Sangawar, *Int. J. Sci. Res. (IJSR)*, **6**: 361 (2017); https://scholar.google.com/citations?view_op=view_citation&hl=en&user=z

FEcjgQAAAAJ&citation_for_view=zFEcjgQAAAAJ:eQOLeE2rZwMC
37. R. S. Abdul Hamza and M. A. Habeeb, *Optical and Quantum Electronics*, **55**, Iss. 8: 705 (2023); https://doi.org/10.1007/s11082-023-04995-3
38. A. Goswami, A. K. Bajpai, and B. K. Sinha, *Polym. Bull.*, **75**, No. 2: 781 (2018); https://doi.org/10.1007/s00289-017-2067-2
39. S. M. Mahdi and M. A. Habeeb, *AIMS Materials Science*, **10**, No. 2: 288 (2023); doi:10.3934/matersci.2023015
40. O. E. Gouda, S. F. Mahmoud, A. A. El-Gendy, and A. S. Haiba, *Indonesian Journal of Electrical Engineering*, **12**, No. 12: 7987 (2014); https://doi.org/10.11591/telkomnika.v12i12.6675
41. M. A. Habeeb and R. S. A. Hamza, *Indonesian Journal of Electrical Engineering and Informatics*, **6**, No. 4: 428 (2018); doi:10.11591/ijeei.v6i1.511
42. N. K. Al-Sharifi and M. A. Habeeb, *East European Journal of Physics*, **2**: 341 (2023); doi:10.26565/2312-4334-2023-2-40
43. A. R. Farhadizadeh and H. Ghomi, *Materials Research Express*, **7**, No. 3: 36502 (2020); https://doi.org/10.1088/2053-1591/ab79d2
44. A. A. Mohammed and M. A. Habeeb, *East European Journal of Physics*, **2**: 157 (2023); doi:10.26565/2312-4334-2023-2-15
45. P. Vasudevan, S. Thomas, K. Arunkumar, S. Karthika, and N. Unnikrishnan, *Journal of Materials Science and Engineering*, **73**: 1 (2015); doi:10.1088/1757-899X/73/1/012015
46. Z. S. Jaber, M. A. Habeeb, and W. H. Radi, *East European Journal of Physics*, **2**: 228 (2023); doi:10.26565/2312-4334-2023-2-25
47. L. M. Chaudhari and R. Nathuram, *Bulg. J. Phys.*, **37**: 232 (2010).